ceramics

MDPI

Article

Influence of the Preparation Method on the Physico-Chemical and Sorption Properties of Montmorillonite

Olga Yu. Golubeva *, Elena Yu. Brazovskaya and Yulia A. Alikina

Laboratory of Silicate Sorbents Chemistry, Institute of Silicate Chemistry of Russian Academy of Sciences, Adm. Makarova emb., 2, 199034 St. Petersburg, Russia
* Correspondence: olga_isc@mail.ru; Tel.: +7-812-325-21-11

Abstract: Layered silicates with a montmorillonite structure are widely used in various fields related to adsorption, gas and water treatment, catalysis, cosmetology and medicine. Under conditions of directed hydrothermal synthesis, montmorillonites with the specified characteristics can be obtained. The influence of the preparation method for montmorillonites of two compositions ($Mg_3Si_4O_{10}(OH)_2$ H_2O and $Na_{1.5}Al_{0.5}Mg_{1.5}Si_4O_{10}(OH)_2$ H_2O) on their sorption properties, moisture absorption, porous textural characteristics and surface properties has been studied. The nature of the initial reagents, the pH of the reaction medium and the synthesis temperature were chosen as the variable synthesis parameters. It has been established that the synthesis conditions significantly affect the properties of montmorillonite, which, in turn, determines the possibilities of using the materials obtained in specific areas.

Keywords: montmorillonite; hydrothermal synthesis; methylene blue; water adsorption; zeta potential; catalysis; medicine

Citation: Golubeva, O.Y.; Brazovskaya, E.Y.; Alikina, Y.A. Influence of the Preparation Method on the Physico-Chemical and Sorption Properties of Montmorillonite. *Ceramics* **2023**, *6*, 922–934. https://doi.org/10.3390/ceramics6020054

Academic Editor: Sergey Mjakin

Received: 27 February 2023
Revised: 28 March 2023
Accepted: 29 March 2023
Published: 3 April 2023

1. Introduction

Minerals with a montmorillonite structure are widely used in various industries—as sorbents for water and gas purification, desiccants, fillers of polymer-inorganic nanocomposites, catalysts and catalyst carriers, as well as sorbents for medical purposes [1–7].

Montmorillonite (MT) is a clay mineral belonging to the smectite group. The crystal structure of these minerals consists of layers built from three sheets—two tetrahedral silicon–oxygen sheets and an octahedral brucite or gibbsite sheet placed between them. Between the layers there can be water molecules and exchange cations. The MT layers have a symmetrical structure and are facing each other with like-charged oxygen atoms, as a result of which the silicon–oxygen networks and aluminum(magnesium)–oxygen–hydroxyl networks are held by van der Waals forces.

A distinctive feature of layered silicates with the structure of montmorillonite (MT) is the ability to intercalate polar liquids with expansion of the interlayer space and subsequent exfoliation into separate layers. This property of montmorillonite is actively used, for example, in the development of polymer-inorganic nanocomposites. A surge in interest in polymer-inorganic nanocomposites is associated with the work of scientists at the Toyota Research Center, who, starting in 1987 [8,9], published a series of articles containing the results of studying nanocomposites based on nylon and clay minerals. It has been found that small additions of layered silicates exfoliated in a polymer matrix into separate layers of nanoscale thickness led to a significant increase in thermal stability and improved the mechanical characteristics of the polymer. Since then, interest in polymer nanocomposites has been constantly growing. This is due to the possibility of a significant improvement in a number of physical and mechanical properties compared to micro- and macro-composites containing the same amount of inorganic filler. The ability of MT to adsorb heavy metals, organic cations, toxins, bacteria, etc., is also actively used in the development of sorbents

for technical and medical purposes (for example, [10–13]). The direction associated with the ability of montmorillonite to absorb mycotoxins is extremely interesting, which makes it in demand in agriculture [14,15]. The possibility of using MT as a catalyst in the synthesis of RNA and DNA is being studied [16–18].

At the same time, raw minerals are complex and unstable multicomponent systems. Their physical and chemical properties significantly depend on the content of the main phase in the rock, the type of cation-exchange form and the nature of impurities. These circumstances limit the wider use of clay minerals in a number of areas, especially in those where the constancy of the structural and physicochemical characteristics of the materials used is necessary, for example, to solve a number of urgent problems in medicine and catalysis. In addition, the diversity of the composition, structural and textural characteristics of natural minerals does not allow for fundamental studies of the effect of structural and physicochemical parameters of materials on their sorption, catalytic and other practically significant properties. In this regard, the problem of obtaining and optimizing methods for the synthesis of montmorillonite with desired characteristics under conditions that allow for their industrial implementation becomes topical.

Many attempts have been made to obtain synthetic MT (for example, [19–23]), but only a few works describe the preparation of a single-phase product with the structure of montmorillonite. In most studies, the synthesis of MT was carried out at temperatures from 150 to 450 °C and autogenous pressure up to 150 MPa. However, there are exceptions. The authors of [24] carried out MT synthesis at low temperatures (from 3 to 20 °C) via co-precipitation of aluminum and magnesium hydroxides with the addition of silica. Depending on the composition of the initial solution, amorphous substances, $Al(OH)_3$ or $Mg(OH)_2$ or a mixture of various phyllosilicates (MT, illites and chlorites) were obtained. The main requirements for the reaction medium for MT synthesis were formulated: 1. pH of the medium must be alkaline or neutral. 2. A low concentration of silicon is required (unsaturated solution with respect to amorphous silicon). 3. The MgO content must be at least 6 wt.%. Such conclusions are consistent with the processes that occur during the formation of MT in nature. Raw MTs are formed during the weathering of alkaline (basic) or acidic rocks of volcanic origin. The most important factor is the composition of the rock, namely the content of magnesium and alkalis in it. From alkaline rocks with a high magnesium content, the formation of MT is possible under alkaline or neutral conditions. From acidic igneous rocks with low magnesium content, natural MTs form only under alkaline pH conditions.

Nevertheless, some works have shown the possibility of MT synthesis under slightly acidic pH conditions (4–6). The authors of [25,26] obtained aluminum–magnesium MT by hydrothermal treatment of hydrogels obtained from acetates of the corresponding metals and SiO_2 in an HF medium.

An analysis of the available literature data shows that synthetic MTs usually require high temperatures (300–400 °C), autogenous pressure to achieve a higher degree of purity and crystallinity of the final product in an acceptable period of time. In addition, the nature of the starting reagents and the pH of the reaction medium can have a great influence. Thus, the use of acetates of the corresponding metals as initial reagents makes it possible to significantly reduce the synthesis temperature to 220–250 °C; however, the physicochemical properties of the final product may differ from the properties of montmorillonite obtained by other methods [27].

An analysis of the works available in the literature allows us to distinguish three main approaches to the synthesis of montmorillonite, which make it possible to obtain a single-phase product of a sufficiently high quality:

1. Hydrothermal treatment of hydrogels of the appropriate composition at temperatures of 300–350 °C in a neutral environment (pH = 7)
2. Hydrothermal treatment of a mixture of acetates of the corresponding metals and SiO_2 at a temperature of 200–250 °C in a slightly acidic medium (pH = 4–6)

3. Hydrothermal treatment of a mixture of the corresponding oxides at a temperature of 300–350 °C in an alkaline medium, pH = 9–10.

The available numerous experimental data are unsystematic, which makes it impossible to determine the optimal technology for obtaining single-phase montmorillonite and to establish the effect of synthesis conditions on practically significant characteristics, such as particle size, specific surface area, surface properties, cation exchange capacity and a number of others. In this paper, an attempt is made to eliminate this gap and to identify the main patterns of the influence of production conditions on the practically important characteristics of montmorillonite.

2. Materials and Methods

2.1. Reagents

The following reagents were used for the synthesis and analysis of the samples: tetraethoxysilane ($(C_2H_5O)_4Si$, special purity grade, ≥99.0%, Sigma, Stainheim, Germany), magnesium nitrate $Mg(NO_3)_2$ $6H_2O$, reagent grade, Vecton, Saint Petersburg, Russia), aluminum nitrate $Al(NO_3)_3 \cdot 9H_2O$ (reagent grade, ≥97.0%), ammonia NH_4OH (25 wt% NH_3 in H_2O), ethanol C_2H_5OH (96 wt%), sodium acetate ($NaCOOCH_3$, 99%, Fluka, Darmstadt, Germany), magnesium acetate ($Mg(COOCH_3)_2$ $4H_2O$, 99%, Fluka, Darmstadt, Germany), aluminum oxide (Al_2O_3, 95%, NevaReaktiv, Saint Petersburg, Russia), silica gel (SiO_2 nH_2O, NevaReaktiv, Saint Petersburg, Russia), magnesium oxide (MgO, NevaReaktiv, Saint Petersburg, Russia), methylene blue $C_{16}H_{18}N_3SCl$ (chemically pure grade, Vecton, Saint Petersburg, Russia), hydrochloric acid HCl (35–38 wt%, NevaReactiv, Saint Petersburg, Russia), sodium nitrate ($NaNO_3$, ACS reagent, ≥99.0%, Sigma, Stainheim, Germany) and sodium hydroxide solution (50 wt% in water, Fluka, Darmstadt, Germany).

2.2. Synthesis

For the synthesis of montmorillonite samples, three main approaches were used, the conditions of which are presented in Table 1. All samples were obtained as a result of hydrothermal treatment of various initial reagents. Mixtures of metal acetates and oxides, dried aluminosilicate gels of the corresponding compositions and mixtures of the corresponding oxides were used as initial precursors subjected to hydrothermal treatment. The initial reagents were taken in stoichiometric ratios corresponding to the formulas of the corresponding samples. We synthesized two compositions of montmorillonite, corresponding to the general chemical formula $Na_{2x}(Al_{2(1-x)},Mg_{2x})Si_4O_{10}(OH)_2$ nH_2O ($0 < x \leq 1$): with x = 1 (composition without aluminum, analog of natural saponite $Mg_3Si_4O_{10}(OH)_2$ H_2O) and x = 0.75 ($Na_{1.5}Al_{0.5}Mg_{1.5}Si_4O_{10}(OH)_2$ H_2O).

Table 1. Preparation conditions and sample compositions.

Synthesis Method Designation	Sample Designation	Samples (Composition by Synthesis)	Synthesis Conditions			
			Reagents	pH	T, °C	Processing Time, Days
1	MT-Al0-ac	$Mg_3Si_4O_{10}(OH)_2$ nH_2O	$Mg(COOCH_3)_2$ $4H_2O$, $NaCOOCH_3$ Al_2O_3, SiO_2	4–5	220	4–5
	MT-Al0.5-ac	$Na_{1.5}Al_{0.5}Mg_{1.5}Si_4O_{10}(OH)_2$ H_2O				
2	MT-Al0 gel	$Mg_3Si_4O_{10}(OH)_2$ nH_2O	Dried hydrogels of the appropriate composition	7	350	3–4
	MT-Al0.5 gel	$Na_{1.5}Al_{0.5}Mg_{1.5}Si_4O_{10}(OH)_2$ H_2O				
3	MT-Al0-ox	$Mg_3Si_4O_{10}(OH)_2$ nH_2O	MgO, SiO_2, Al_2O_3 $NaNO_3$	7–9	350	3–4
	MT-Al0.5-ox	$Na_{1.5}Al_{0.5}Mg_{1.5}Si_4O_{10}(OH)_2$ H_2O				

Hydrogels of the corresponding compositions were prepared according to the procedure described in [23]. Aluminum, magnesium and sodium nitrates were dissolved in the required amounts in nitric acid with the addition of ethanol, tetraethoxysilane was poured into the resulting mixture and precipitation was carried out with an ammonia solution. The

resulting gel was dried at 100 °C for 30 h and then calcined at 500 °C for 1 h to decompose nitrates, remove water and organic compounds and form a gel based on the corresponding oxides. The starting reagents and dried gels were subjected to hydrothermal treatment in steel autoclaves with Teflon crucibles at appropriate temperatures, filling factor 0.8. The crystallization products were washed with distilled water and dried at 80 °C for 12 h.

2.3. Characterization

X-ray phase analysis of the samples was carried out using a powder diffractometer Rigaku Corporation, SmartLab 3 (CuKα—radiation, operating mode—40 kV/40 mA; semiconductor point detector (0D)—linear (1D), θ-θ geometry, measurement range 2ϑ = 5–70° (step 2θ = 0.01°)).

Chemical analysis of the samples for the content of Si and Al was carried out using the gravimetric method using quinolate of a silicon–molybdenum complex and by complexometric titration at pH 5. Loss on ignition и content of H_2O was estimated from the weight loss upon calcination of the sample at 1000–1100 °C. The sodium content in the samples was determined by flame photometry on an iCE3000 atomic absorption spectrometer.

The morphology of the samples was studied by scanning electron microscopy (SEM) by using a Carl Zeiss Merlin instrument (Oberkochen, Germany) with a field-emission cathode. Powders of the samples were planted directly on conductive carbon tape without additional processing.

The porous structure was analyzed based on the low-temperature nitrogen sorption method (Quantachrome NOVA 1200e, USA; relative pressure range: 0.005–0.999 P/P_o, pressure resolution 0.0015%). Degassing was performed at 300 °C for 12 h. The specific surface area of the sample was calculated using the BET method [28] using NOVAWin (USA) software. The relative error in the specific surface area value was 1%.

The electrokinetic (zeta) potential of the samples was determined using a particle size and zeta potential analyzer NaniBrook 90 PlusZeta (Brookehaven Instruments Corporation, Holtsville, NY, USA). The samples were a suspension obtained by dispersing 50 mg of sample in 20 mL of deionized water. Before measurements, the suspension was subjected to low-power (50 W) ultrasonication for two minutes on an ultrasonic processor UP50H.

The functional composition of the sample surface was studied via the method of adsorption of acid–base indicators with different pKa values in a range from −4.4 to 14.2, undergoing selective adsorption on the surface of active centers with the corresponding pKa values, according to the procedure described in [29]. The content of adsorption centers was determined from the change in the optical density of aqueous solutions of indicators using UV absorption spectroscopy (LEKISS2109UV spectrophotometer).

The moisture absorption capacity of the samples was determined under static conditions at a temperature of (20 ± 1) °C at various relative water vapor pressures. The pre-tested samples were dehydrated in an oven for two hours at a temperature of 200 °C. The moisture absorption kinetics were studied in a wide range of relative water vapor pressures from 0.18 to 0.95. A dried sample of 100 mg was placed in the boat of the torsion balance. Under the boat, there was a container with a saturated solution of various salts, providing a given value of p/p_s of water vapor. The change in the mass of the sample in the boat was recorded on a scale of torsion balances depending on the saturation time. Upon reaching the value of weight gain, which does not change for 1 h, the experiment was stopped, and the last weight gain was considered to be equilibrium for this p/p_s. The adsorption capacity was determined by the difference in the mass of the adsorbent sample before and after saturation to an equilibrium state, referred to as the initial mass of the dehydrated sample.

The adsorption capacity of the samples was determined with respect to the cationic organic dye—methylene blue (MB). The study of the equilibrium adsorption of MB was carried out at a concentration of MB in a range from 10 to 400 mg/L. To achieve this, 20 mg of the sample was dispersed in 20 mL of an aqueous dye solution. The experiments were carried out in static mode at room temperature in closed glass bottles with a volume of

50 mL with stirring for 120 min, which corresponded to the moment when adsorption equilibrium was established. The samples were filtered, and the concentration of dyes in the filtrate was determined as the arithmetic mean of three measurements. The concentration of MB was determined using UV absorption spectroscopy (LEKISS2109UV spectrophotometer, SHIMADZU UV-2600/2700) via optical density at a wavelength of 246 nm [30].

The capacity of the sorbent, mg/g (the amount of adsorbed substance) was determined using Formula (1):

$$X = \frac{\left(C_i - C_f\right) \cdot V_s}{m_s} \quad (1)$$

where C_i is the initial concentration of MB solution, g/L; C_f—final concentration after sorption, g/l; V_s is the volume of MB solution, L; m_s—weight of the sorbent sample, g.

3. Results and Discussion

3.1. Phase and Chemical Composition of the Samples

The most important characteristic affecting the possibility of using a material in areas, such as medicine or catalysis, is its phase purity. X-ray diffraction patterns of the samples are shown in Figure 1. Samples of trioctahedral layered silicates of the montmorillonite subgroup were obtained, as evidenced by the position of the *hkl* reflection peaks characteristic of montmorillonite and saponite mineral at 7–10° (001), 19° (110), 28° (004), 35° (201), 53 (210) and 61° (060) [31].

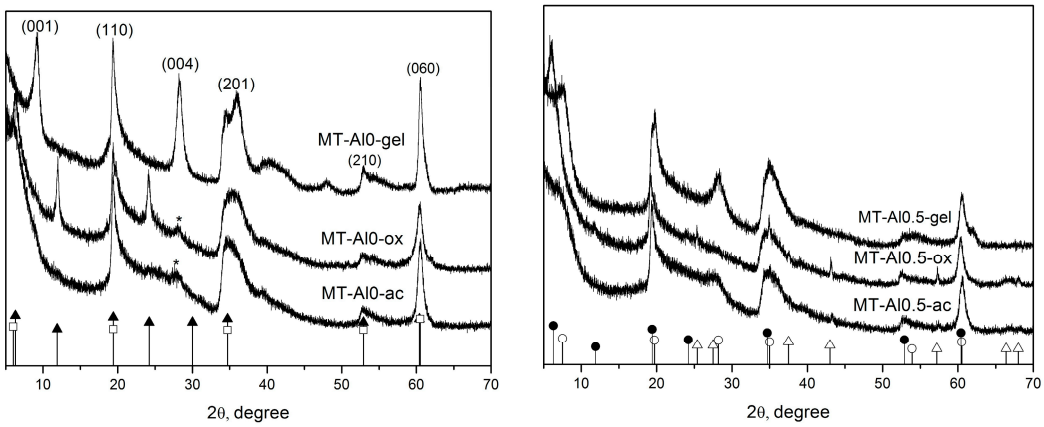

Figure 1. X-ray diffraction patterns of the samples: (**a**)—Al0 compositions; (**b**)—Al0.5 compositions. Bar chart of the standards: *—quartz (PDF № 79-1913); ▲—Saponite 15 Å (PDF № 13-86); △—Al_2O_3 (PDF № 50-1496); □—Sap-15 Å Al-rich (PDF №30-789); ●—raw montmorillonite (PDF No. 48-74), ○–montmorillonite.

The mineral saponite belongs to the group of trioctahedral magnesium smectites in the montmorillonite subgroup. It can be considered as a limiting case of montmorillonite $Na_{2x}(Al_{2(1-x)},Mg_{2x})Si_4O_{10}(OH)_2\ nH_2O$ with $x = 1$. Sometimes, in raw saponites, there are isomorphic substitutions of a part of silicon Si^{4+} in tetrahedral layers for aluminum Al^{3+}.

The reflection in the region of angles 2θ = 6–9 (d_{001}) characterizes the basal space between the silicon–oxygen sheets in the structure of montmorillonite. Thus, the position of the reflection on the diffraction pattern of magnesium montmorillonite MT-Al0 in the region of angles 2θ = 9.2 corresponds to an interlayer distance of 9.6 Å, a shift in the reflection for the MT-Al0 gel sample to the region of small angles 2θ = 7.1 indicates an increase in the interlayer distance to 12.4 Å. The reflections in the diffraction patterns are rather broad and asymmetric, which indicates a disordered structure and a high dispersion of the crystals. For the MT-Al0-ac and MT-Al0.5-ac patterns, the d_{001} peak is absent. The broadening and disappearance of the reflection peak (001) are associated with the loss of periodicity along the *c* axis and indicate a disordered packing of montmorillonite layers. It

is known that montmorillonite packets are formed from layers, from which the secondary structure of montmorillonite is then formed, which can be seen in the electron micrographs of the samples shown in Figure 2.

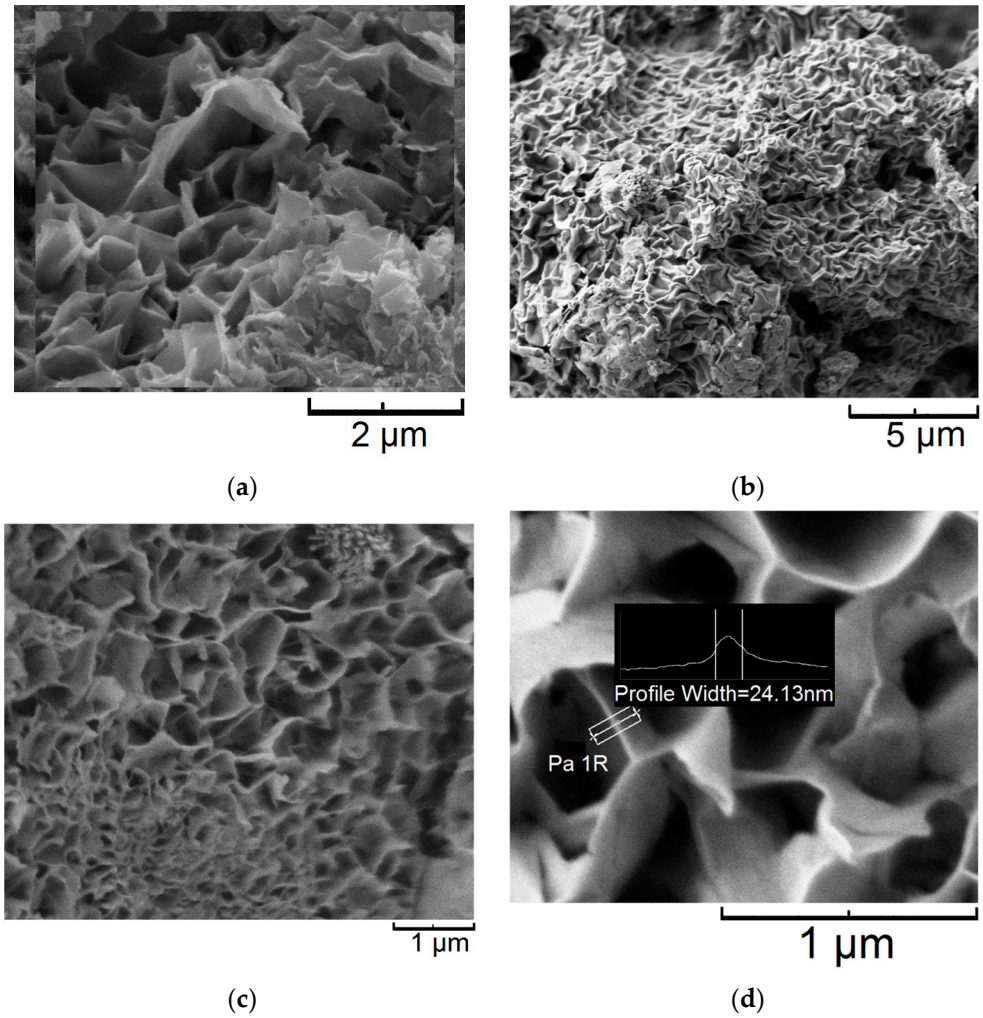

Figure 2. SEM images of the samples: (**a**)—MT-Al0.5 gel; (**b**)—MT-Al0 gel; (**c**,**d**)—MT-Al0-ac. Samples are designated in accordance with the designations presented in Table 1.

Some samples contain impurity phases of silicon and aluminum oxides in insignificant amounts. This primarily applies to samples synthesized from oxides of the corresponding elements using method 3 (see Table 1). Impurity phases are also contained in very small amounts in the samples obtained by method 1. The samples obtained by method 2 are single-phase and do not contain impurity phases.

It should be noted that there is a significant decrease in the synthesis temperature when using method 1—from 350 °C (methods 2 and 3) to 220 °C. As shown earlier [32], at synthesis temperatures below 350 °C using method 2, the degree of crystallinity of montmorillonite decreases significantly, and at temperatures of 200 °C, it practically does not crystallize. The use of method 3 at temperatures lower than 350 °C leads to an increase in the amount of impurity phases and a decrease in the yield of montmorillonite.

Previously, the process of crystallization of montmorillonite with the composition $Mg_3Si_4O_{10}(OH)_2$ nH_2O from oxides in an alkaline medium was studied [33]. The influence of the synthesis temperature, the duration of synthesis and the concentration of sodium hydroxide solution, which acts as a reaction medium, on the nature of montmorillonite crystallization was studied. It was found that in all cases, MT crystallizes with significant impurities in the brucite phase and, in some cases, phases of magnesium hydroxide and

silicon oxide. The present work shows the possibility of obtaining montmorillonite with a small amount of an impurity phase through hydrothermal treatment of the corresponding oxides in a neutral medium at a temperature of 350 °C for three to four days.

Thus, the approach using dried gels of the corresponding composition as starting reagents subjected to hydrothermal treatment (method 2) can be considered optimal from the point of view of obtaining single-phase products with a montmorillonite structure. The gel is highly reactive, homogeneous and free of any crystal structures, which allows for faster synthesis time and avoids impurities.

The results of the chemical analysis of the samples presented in Table 2 confirm that aluminum–magnesium hydro-silicates have been obtained. The results of studying the samples using scanning electron microscopy (Figure 2) show that all samples have a layered particle morphology characteristic of montmorillonites.

Table 2. Results of chemical analysis of the samples.

Sample	Chemical Composition, wt.%				
	SiO_2	Al_2O_3	MgO	Na_2O	Loss on Ignition, %
MT-Al0-ac	59.1	-	21.0	0.04	13.1
MT-Al0 gel	61.2	-	32.2	0.02	6.6
MT-Al0-ox	52.6	-	27.3	0.13	12.9
MT-Al0.5-ac	52.7	7.5	11.7	4.47	17.4
MT-Al05 gel	58.1	13.8	13.1	2.76	8.9
MT-Al0.5-ox	57.3	10.8	16.2	0.20	11.0

3.2. Porous Textural Characteristics of the Samples

The porous textural characteristics and surface properties are very important characteristics of both sorption materials and catalysts. Table 3 presents the porous textural characteristics of the samples and the results of the evaluation of their surface zeta potential. The surface of all samples is negatively charged, which is a characteristic feature of aluminosilicates. The specific surface area is largely determined by the conditions of sample synthesis. Thus, for samples obtained using method 2, it is the largest and reaches 180 m^2/g or more. The smallest specific surface area of the samples obtained by method 3 is 77–80 m^2/g, depending on the composition of the sample.

Table 3. Specific surface area and zeta potential of the sample surface.

Sample	SSA [a], m^2/g	n	ζ-Potential, mV
MT-Al0 gel	188 ± 15	4	−11.8 ± 1.9
MT-Al0-ac	134 ± 7	6	−10.3 ± 0.6
MT-Al0-ox	84.7 ± 12	10	−18.6 ± 2.5
MT-Al0.5 gel	184 ± 15	4	−25.4 ± 0.8
MT-Al0.5-ac	89.3 ± 11	9.5	−22.5 ± 2.2
MT-Al0.5-ox	67.4 ± 8	13	−17.2 ± 2.6

[a]-SSA—specific surface area (m^2/g).

The average particle size of the synthesized montmorillonites, determined from X-ray diffraction data, is 40 ± 7 nm. The particle size was calculated using the Scherrer formula using the reflection band 2θ = 19° (110), which characterizes the particle size in the plane perpendicular to the *c* axis. At the same time, knowing the specific surface area, one can estimate the average number of layers (n) forming a layered silicate particle using the formula proposed in [34]: $S(_M{}^2/_\Gamma) = 801.3/n + 5.13$. The results of the calculations according to the given formula showed that for synthesized samples, the number of layers may vary from 4 to 13, depending on the composition and conditions of the synthesis.

3.3. Desiccant Capacity of the Samples

The ability to absorb moisture largely determines the possibility of using materials as desiccants and absorbers of liquids of various nature. The ability to absorb moisture largely determines the possibility of using materials as desiccants. Figure 3 presents the results of a study of the absorption of water vapor under study. The greatest moisture content is in MT-Al0.5 samples obtained by methods 1 and 2. With maximum values of p/p_s 0.99, the moisture content of these samples reaches 55–57%. Small moisture content is characterized by sample Al0-ac (50% with p/p_s 0.99). Samples obtained using method 3 demonstrate the lowest moisture content in a series of samples of the same chemical composition obtained by other methods.

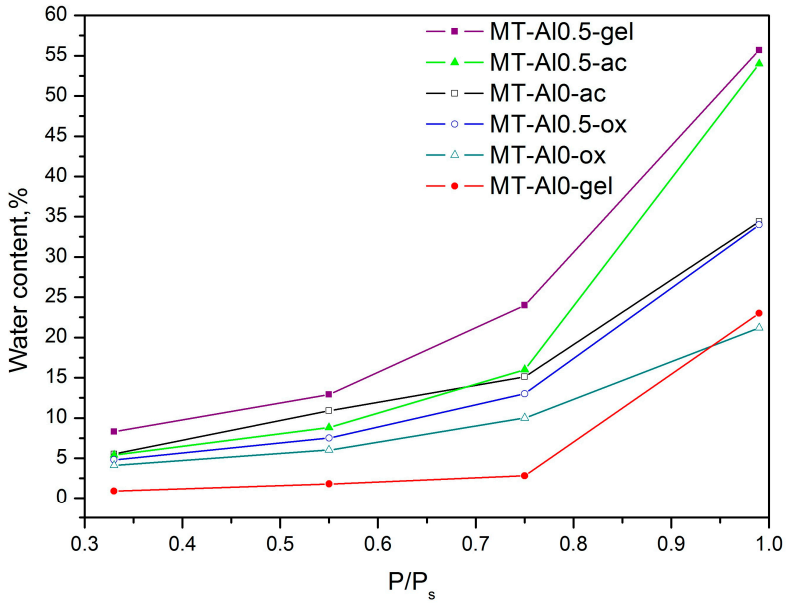

Figure 3. Moisture adsorption isotherms.

The results show that the moisture capacity of MTs is determined via the chemical composition of samples—aluminum-containing samples, as a whole, have greater moisture content than compounds without aluminum. An exception is the composition of the MT-Al0-ac composition, demonstrating a fairly high degree of adsorption of water vapor, even exceeding such for aluminum-containing composition MT-Al0.5-ox. Connections between the specific surface of the samples and their moisture content were not found. A sample with the largest specific surface of MT-Al0 gel is characterized by the smallest absorption ability, and the MT-Al0.5 gel with the same specific surface shows the greatest absorption ability.

3.4. Distribution of Active Sites on the Surface

The distribution of active sites on the surface of solids is important for both potential catalysts and sorbents. The distribution of the adsorption sites on the surface of the studied samples as a function of their pKa values is shown in Figure 4. It is known that the properties of a solid surface are determined not only by the chemical nature of the substance but also depend on the method of preparing the sample, its dispersion and porosity, which demonstrate the presented results. Results obtained indicate the presence of different types of adsorption centers on the surface all samples, including Lewis base (pKa $\leq$ 0, formed by oxygen atoms) and acidic (pKa $\geq$ 14, formed by silicon atoms) as well as Brønsted acidic (0 < pKa < 6), neutral (pKa~6–8) and basic (8 < pKa < 14) sites, corresponding to hydroxyl groups [29]. Moreover, the number of certain centers on the surface of the samples is different, depending on the sample composition and their synthesis method.

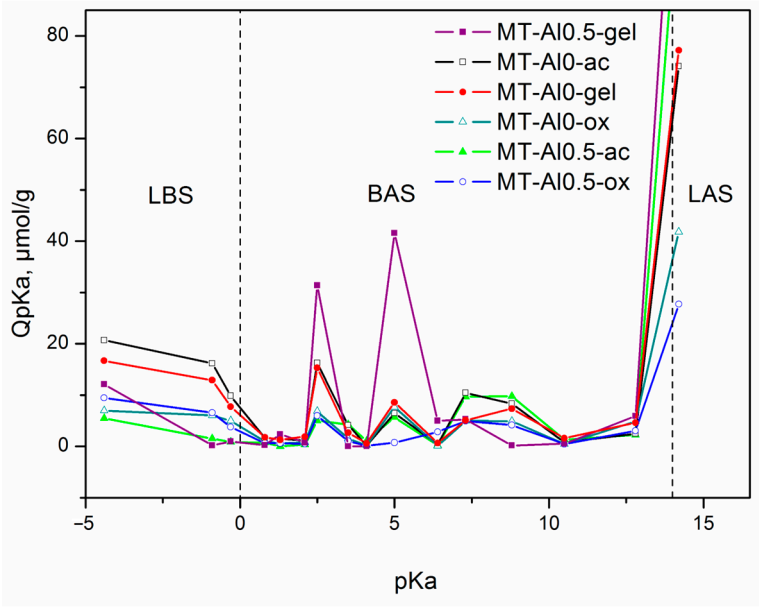

Figure 4. Distribution of the adsorption centers as a function of their pKa values on the surface of samples. LBS—Lewis basic sites; BAS—Brønsted acidic sites; LAS—Lewis acidic sites.

The largest number of Brønsted and Lewis acid centers is characteristic of the MT-Al0.5 gel sample. Many Brønsted acid centers are also characteristic of the samples of MT-Al0-ac and MT-Al0 gel. For all samples obtained by method 3, the amount of acid centers is low. Despite the fact that the number of Lewis acid centers on the MT surface is not as large as the zeolites [35,36], montmorillonites are actively used in heterogeneous catalysis [6,37]. Therefore, we can conclude that method 2 contributes to the formation of more active centers on the MT surface and, therefore, can be used to obtain effective heterogeneous montmorillonite catalysts.

3.5. Methylene Blue Adsorption

Methylene blue (MB) is a cationic dye that is quite well sorbed by aluminosilicates that carry a negative [38–42]. At the same time, MB can act as a model compound, which makes it possible to evaluate both the ability of the material to be used as a sorbent for wastewater treatment from organic contaminants [43] and as a medical sorbent. Methylene blue can be considered as a simulant of medium-molecular-weight toxins, and the possibility of using materials as enterosorbents can be assessed [44].

Figure 5 shows MB adsorption isotherms by synthetic montmorillonites. The MT-Al0.5 gel sample has the greatest sorption capacity, and the MT-Al0 gel sample is characterized by the lowest levels of sorption capacity. At the same time, the Al0 composition, obtained by method 1 (MT-Al0-ac), also has a fairly high sorption capacity approaching the values of the MT-Al0.5 gel sample. Thus, we can conclude that the method of obtaining samples has the greatest effect on their physico-chemical and operational characteristics.

A comparative study of the applicability of the adsorption models of Langmuir, Freindlich and Dubinin–Radushkevich [45–48] was carried out. The parameters of the adsorption equations were calculated by the method of nonlinear regression using the OriginPro 8 program. The constants and parameters of all equations are given in Table 4. By comparing the correlation coefficients, it was shown that the Freundlich model best describes adsorption on all MT-Al0 samples. According to this model, the surface of the studied sorbents contains active centers with different energies of affinity for dye molecules. A value of 1/n can be considered as an indicator of the inhomogeneity of sorption centers: as the inhomogeneity increases, $1/n \rightarrow 0$, and as the homogeneity of centers increases, $1/n \rightarrow 1$. At the same time, the data obtained make it possible to characterize aluminosilicates as materials with a high concentration of sorption centers with different degrees of activity.

The constant K_F has a linear dependence on the adsorption capacity of the adsorbent, i.e., the larger this constant, the greater the adsorption capacity.

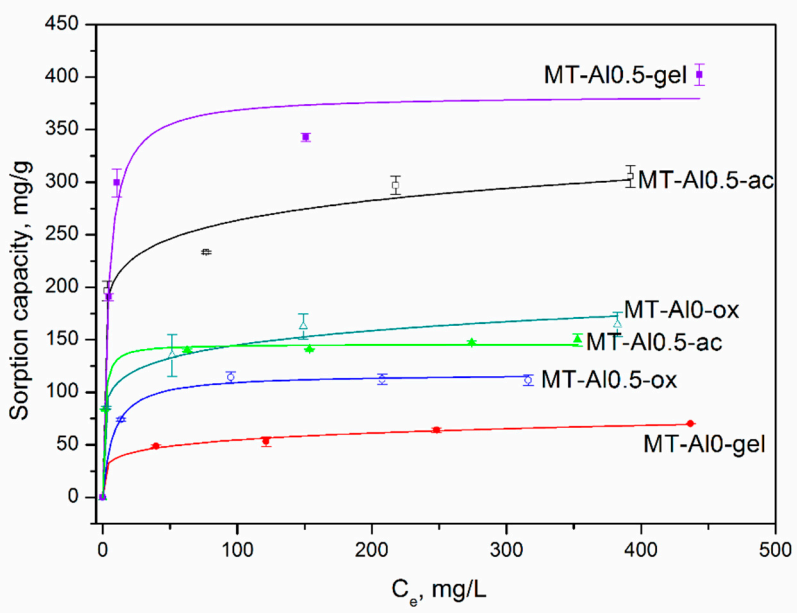

Figure 5. Methylene blue adsorption isotherms. Langmuir isotherms: MT-Al0.5 gel, MT-Al0.5-ox, MT-Al0.5-ac Freundlich isotherms: MT-Al0 gel, MT-Al0-ox, MT-Al0-ac.

Table 4. Equation constants of methylene blue adsorption isotherms.

Samples Morphology	q_{exp}	Langmuir Equation			Freundlich Equation			Dubinin-Radushkevich			
		q_m	K_L,	R^2	n	K_F	R^2	q_m	β	E	R^2
Al0 gel	70 ± 1	69 ± 4	(5.1 ± 0.2) × 10^{-2}	0.97	6.1 ± 0.8	25 ± 3	0.99	63 ± 2	7.2 ± 0.1	0.30 ± 0.06	0.6
Al0-ox	164 ± 11	158 ± 7	0.45 ± 0.1	0.97	7.7 ± 1.1	80 ± 7	0.98	202 ± 15	(1.1 ±0.2) × 10^{-3}	21 ± 1	0.97
Al0-ac	305 ± 10	282 ± 18	0.7 ± 0.3	0.94	10 ± 2	166 ± 17	0.98	411 ± 34	(5.0 ± 0.1) × 10^{-3}	10 ± 2	0.97
Al0.5 gel	402 ± 10	383 ± 20	(2.5 ± 0.7) × 10^{-2}	0.97	8 ± 2	190 ± 29	0.95	459 ± 22	(5.0 ± 0.1) × 10^{-3}	10 ± 1	0.95
Al0.5-ox	111.5	117 ± 3	(1.3 ± 0.2) × 10^{-2}	0.99	8 ± 3	58 ± 12	0.97	154 ± 9	6.7 ± 0.2	0.30 ± 0.02	0.99
Al0.5-ac	150 ± 5	145 ± 28	(8.4 ± 0.8) × 10^{-2}	0.99	9 ± 1	84 ± 6	0.98	182 ± 33	9.6 ± 0.5	0.20 ± 0.04	0.99

q_m—maximum sorption capacity (mg/g), q_{exp}—experimental value of sorption capacity (mg/g); K_L—Langmuir constant related to adsorption free energy (L/g); K_F—Freundlich constant related to adsorbent capacity; β—the Dubinin–Radushkevich isotherm constant, $mol^2/(K^2 \cdot J)$; E—the adsorbate energy per molecule as the energy needed to remove molecules from the surface, kJ/mol.

Taking into account the high values of the correlation coefficients (R^2) and close values of the experimental and calculated sorption capacities, the Langmuir isotherm most adequately describes adsorption on all MT-Al0.5 samples. This model describes a homogeneous monomolecular adsorption process and assumes that the surface of a solid body contains a finite number of active centers with equal energy.

The Dubinin–Radushkevich isotherm model was used to determine the equation constants, which were subsequently used to calculate the free energy of methylene blue adsorption on the studied samples. The energy values were in a range from 0.2 to 22 kJ/mol. Based on this, it was concluded that the process of dye sorption proceeds according to the mechanism of physical adsorption (physical adsorption E = 10–30 kJ/mol, chemical adsorption—the energy of chemical adsorption reaches several hundred kJ/mol).

In the Supplementary Information file the results of an additional study of the kinetics of methylene blue adsorption using pseudo-first order (PFO) and pseudo-second order PSO) adsorption models (Figures S1 and S2, Table S1) [49–51].

4. Conclusions

Samples with a montmorillonite structure of two compositions (**$Mg_3Si_4O_{10}(OH)_2$ H_2O** and $Na_{1.5}Al_{0.5}Mg_{1.5}Si_4O_{10}(OH)_2$ H_2O) were obtained under hydrothermal conditions using three different approaches—hydrothermal treatment of hydrogels of the appropriate composition at temperatures of 300–350 °C in a neutral environment (pH = 7), hydrothermal treatment of a mixture of acetates of the corresponding metals and SiO_2 at a temperature of 200–250 °C in a slightly acidic medium (pH = 4–6) and hydrothermal treatment of a mixture of the corresponding oxides at a temperature of 300–350 °C in an alkaline medium with pH = 9–10. It was established that the properties of samples are largely determined by their chemical composition; however, the method of obtaining samples has the greatest effect on their properties. Samples of the same composition obtained by various methods can vary significantly in their properties. The hydrogel crystallization method allows one to obtain single-phase samples with a high specific surface, which is probably associated with the porous structure, amorphous and uniformity of the original gel. However, this method is not suitable for obtaining magnesium–silicate samples of the $Mg_3Si_4O_{10}(OH)_2$ H_2O composition, is multistage and cannot be attributed to environmentally friendly and resource-saving ones, as it requires quite high temperatures, as well as the use of toxic reagents (ammonia and tetraethoxysilane). At the same time, the high value of sorption capacity, moisture absorption, the number of active centers on the surface, as well as the phase purity of the resulting product allows us to recommend this method of montmorillonite obtaining for its further use in medicine and catalysis, where these indicators are necessary. The method of synthesis from oxides of the corresponding metals can be considered as the simplest, most environmentally friendly and cheap method of montmorillonite synthesis. However, the presence of impurity phases affects the properties of the material obtained using this method. The method of obtaining montmorillonite by using the hydrothermal treatment of the acetates of the corresponding metals in a weak acid medium allows one to obtain single-phase montmorillonite $Mg_3Si_4O_{10}(OH)_2$ H_2O at a significantly lower temperature (200–250 °C), with sufficiently high values of moisture absorption and sorption capacity. This method can be considered a way of obtaining sorbents and dehumidifiers for technical purposes.

Supplementary Materials: The following supporting information can be downloaded at: https://www.mdpi.com/article/10.3390/ceramics6020054/s1, Methylene blue absorption spectra (Figure S1. Absorption spectra and photographs of 200 mg/ mL of MB. Curves 1—before and 2—after addition of montmorillonite samples (*a*) Al0 gel (24 h); (*b*) Al0.5 gel (2 h)), Kinetics of methylene blue adsorption (Figure S2. Kinetic curves of MB adsorption by the montmorillonite samples, Table S1. Parameters of kinetic models of sorption of methylene blue on montmorillonites).

Author Contributions: Conceptualization, O.Y.G.; Methodology, O.Y.G.; Validation, O.Y.G., Y.A.A. and E.Y.B.; Formal Analysis, O.Y.G. and Y.A.A.; Investigation, Y.A.A. and E.Y.B.; Resources, O.Y.G.; Data Curation, O.Y.G., Y.A.A. and E.Y.B.; Writing—Original Draft Preparation, O.Y.G. All authors have read and agreed to the published version of the manuscript.

Funding: The study was conducted with the support of the state assignment of the Institute of Silicate Chemistry RAS (Theme No. 0081-2022-0001).

Institutional Review Board Statement: Not applicable.

Informed Consent Statement: Not applicable.

Data Availability Statement: Not applicable.

Acknowledgments: The authors are grateful to the administration of the St. Petersburg Technological Institute (Technical University) for the opportunity to use the equipment of the Engineering Center (X-ray diffractometer). The authors also express their gratitude to the Department of general chemical technology and catalysis of St. Petersburg Technological Institute (Technical University) for the opportunity to conduct studies on the moisture capacity of the samples.

Conflicts of Interest: The authors declare no conflict of interest.

References

1. Hearon, S.E.; Orr, A.A.; Moyer, H.; Wang, M.; Tamamis, P.; Phillips, T.D. Montmorillonite clay-based sorbents decrease the bioavailability of per- and polyfluoroalkyl substances (PFAS) from soil and their translocation to plants. *Environ. Res.* **2022**, *205*, 112433. [CrossRef] [PubMed]
2. França, D.B.; Oliveira, L.S.; Filho, F.G.N.; Filho, E.C.S.; Osajima, J.A.; Jaber, M.; Fonseca, M.G. The versatility of montmorillonite in water remediation using adsorption: Current studies and challenges in drug removal. *J. Environ. Chem. Eng.* **2022**, *10*, 107341. [CrossRef]
3. Jiang, J.-Q.; Cooper, C.; Ouki, S. Comparison of modified montmorillonite adsorbents: Part I: Preparation, characterization and phenol adsorption. *Chemosphere* **2002**, *47*, 711–716. [CrossRef] [PubMed]
4. Zhu, Y.; Iroh, J.O.; Rajagopolan, R.; Aykanat, A.; Vaia, R. Optimizing the Synthesis and Thermal Properties of Conducting Polymer–Montmorillonite Clay Nanocomposites. *Energies* **2022**, *15*, 1291. [CrossRef]
5. Kumar, B.S.; Dhakshinamoorthy, A.; Pitchumani, K. K10 montmorillonite clays as environmentally benign catalysts for organic reactions. *Catal. Sci. Technol.* **2014**, *4*, 2378–2396. [CrossRef]
6. Takabatake, M.; Motokura, K. Montmorillonite-based heterogeneous catalysts for efficient organic reactions. *Nano Express* **2022**, *3*, 2–13. [CrossRef]
7. Park, J.-H.; Shin, H.-J.; Kim, M.H.; Kim, J.-S.; Kang, N.; Lee, J.-Y.; Kim, K.-T.; Lee, J.I.; Kim, D.-D. Application of montmorillonite in bentonite as a pharmaceutical excipient in drug delivery systems. *J. Pharm. Investig.* **2016**, *46*, 363–375. [CrossRef]
8. Okada, A.; Kawasumi, M.; Usuki, A.; Kojima, Y.; Kurauchi, T.; Kamigaito, O. Nylon 6—Clay hybrid. *MRS Online Proc. Libr.* **1989**, *171*, 45–50. [CrossRef]
9. Okada, A.; Usuki, A. Polymer-layered silicate nanocomposites: An overview. *Macromol. Mater. Eng.* **2006**, *291*, 1449–1476. [CrossRef]
10. Abollino, O.; Aceto, M.; Malandrino, M.; Sarzanini, C.; Mentasti, E. Adsorption of heavy metals on Na-montmorillonite. Effect of pH and organic substances. *Water Res.* **2003**, *37*, 1619–1627. [CrossRef]
11. Rytwo, G.; Nir, S.; Margulies, L. A model for adsorption of divalent organic cations to montmorillonite. *J. Colloid Interface Sci.* **1996**, *181*, 551–560. [CrossRef]
12. Tang, G.; Jia, C.; Wang, G.; Yu, P.; Jiang, X. Adsorption mechanism of bacteria onto a Na-montmorillonite surface with organic and inorganic calcium. *bioRxiv* **2020**. [CrossRef]
13. Olopade, B.K.; Oranusi, S.U.; Nwinyi, O.C.; Lawal, I.A.; Gbashi, S.; Njobeh, P.B. Decontamination of T-2 toxin in maize by modified montmorillonite clay. *Toxins* **2019**, *11*, 616. [CrossRef] [PubMed]
14. Mitchell, N.J.; Xue, K.S.; Lin, S.; Marroquin-Cardona, A.; Brown, K.A.; Elmore, S.E.; Tang, L.; Romoser, A.; Gelderblom, W.C.A.; Wang, J.-S.; et al. Calcium montmorillonite clay reduces AFB1 and FB1 biomarkers in rats exposed to single and co-exposures of aflatoxin and fumonisin. *J. Appl. Toxicol.* **2014**, *34*, 795–804. [CrossRef]
15. Wang, G.; Xu, J.; Sun, Z.; Zheng, S. Surface functionalization of montmorillonite with chitosan and the role of surface properties on its adsorptive performance: A comparative study on mycotoxins adsorption. *Langmuir* **2020**, *36*, 2601–2611. [CrossRef] [PubMed]
16. Ferris, J.P. Montmorillonite-catalyzed formation of RNA oligomers: The possible role of catalysis in the origin of life. *Philos. Trans. R. Soc. London. Ser. B Biol. Sci.* **2006**, *361*, 1777–1786; discussion 1786. [CrossRef] [PubMed]
17. Jheeta, S.; Joshi, P.C. Prebiotic RNA synthesis by montmorillonite catalysis. *Life* **2014**, *4*, 318–330. [CrossRef]
18. Aldersley, M.F.; Joshi, P.C.; Price, J.D.; Ferris, J.P. The role of montmorillonite in its catalysis of RNA synthesis. *Appl. Clay Sci.* **2011**, *54*, 1–14. [CrossRef]
19. Yamada, H.; Nakazawa, H.; Yoshioka, K.; Fujita, T. Smectites in the montmorillonite-beidellite series. *Clay Miner.* **1991**, *26*, 359–369. [CrossRef]
20. Carrado, K.A.; Csencsits, R.; Thiyagarajan, P.; Seifert, S.; Macha, S.M.; Harwood, J.S. Crystallization and textural porosity of synthetic clay minerals. *J. Mater. Chem.* **2002**, *12*, 3228–3237. [CrossRef]
21. Shao, H.; Pinnavaia, T.J. Synthesis and properties of nanoparticle forms saponite clay, cancrinite zeolite and phase mixtures thereof. *Microporous Mesoporous Mater.* **2010**, *133*, 10–17. [CrossRef] [PubMed]
22. Kloprogge, J.T. Synthesis of smectites and porous pillared clay catalysts: A review. *J. Porous Mater.* **1998**, *5*, 5–41. [CrossRef]
23. Golubeva, O.Y.; Ul'yanova, N.Y.; Kostyreva, T.G.; Drozdova, I.A.; Mokeev, M.V. Synthetic nanoclays with the structure of montmorillonite: Preparation, structure, and physico-chemical properties. *Glass Phys. Chem.* **2013**, *39*, 533–539. [CrossRef]
24. Harder, H. The role of magnesium in the formation of smectite minerals. *Chem. Geol.* **1972**, *10*, 31–39. [CrossRef]
25. Reinholdt, M.; Miehé-Brendlé, J.; Delmotte, L.; Tuilier, M.-H.; le Dred, R.; Cortès, R.; Flank, A.-M. Fluorine route synthesis of montmorillonites containing Mg or Zn and characterization by XRD, thermal analysis, MAS NMR, and EXAFS spectroscopy. *Eur. J. Inorg. Chem.* **2001**, *2001*, 2831–2841. [CrossRef]
26. Reinholdt, M.; Miehe-Brendle, J.; Delmotte, L.; Le Dred, R.; Tuilier, M.H. Synthesis and characterization of montmorillonite-type phyllosilicates in a fluoride medium. *Clay Miner.* **2005**, *40*, 177–190. [CrossRef]
27. Golubeva, O.Y. Features of the Hydrothermal Synthesis of Montmorillonite in an Acidic Medium. *Glas. Phys. Chem.* **2018**, *44*, 616–619. [CrossRef]
28. Brunauer, S.; Emmett, P.H.; Teller, E. Adsorption of gases in multimolecular layers. *J. Am. Chem. Soc.* **1938**, *60*, 309–319. [CrossRef]
29. Bardakhanov, S.P.; Vasiljeva, I.V.; Kuksanov, N.K.; Mjakin, S.V. Surface functionality features of nanosized silica obtained by electron beam evaporation at ambient pressure. *Adv. Mater. Sci. Eng.* **2010**, *2010*, 241695. [CrossRef]

30. Ghosh, D.; Bhattacharyya, K.G. Adsorption of methylene blue on kaolinite. *Appl. Clay Sci.* **2002**, *20*, 295–300. [CrossRef]
31. MacEwan, D.M. Identification of the montmorillonite group of minerals by X-rays. *Nature* **1944**, *154*, 577–578. [CrossRef]
32. Golubeva, O.Y. Effect of synthesis conditions on hydrothermal crystallization, textural characteristics and morphology of aluminum-magnesium montmorillonite. *Microporous Mesoporous Mater.* **2016**, *224*, 271–276. [CrossRef]
33. Golubeva, O.Y.; Korytkova, E.N.; Gusarov, V.V. Hydrothermal Synthesis of Magnesium Silicate Montmorillonite for Polymer-Clay Nanocomposites. *Russ. J. Appl. Chem.* **2005**, *78*, 26–32. [CrossRef]
34. Cases, J.M.; Berend, I.; Besson, G.; Francois, M.; Uriot, J.P.; Thomas, F.; Poirier, J.E. Mechanism of adsorption and desorption of water vapor by homoionic montmorillonite. 1. The sodium-exchanged form. *Langmuir* **1992**, *8*, 2730–2739. [CrossRef]
35. Chai, Y.; Dai, W.; Wu, G.; Guan, N.; Li, L. Confinement in a zeolite and zeolite catalysis. *Acc. Chem. Res.* **2021**, *54*, 2894–2904. [CrossRef] [PubMed]
36. Xu, B.; Sievers, C.; Hong, S.B.; Prins, R.; van Bokhoven, J.A. Catalytic activity of Brønsted acid sites in zeolites: Intrinsic activity, rate-limiting step, and influence of the local structure of the acid sites. *J. Catal.* **2006**, *244*, 163–168. [CrossRef]
37. Bonacci, S.; Iriti, G.; Mancuso, S.; Novelli, P.; Paonessa, R.; Tallarico, S.; Nardi, M. Montmorillonite K10: An efficient organo-heterogeneous catalyst for synthesis of benzimidazole derivatives. *Catalysts* **2020**, *10*, 845. [CrossRef]
38. Golubeva, O.Y.; Pavlova, S.V. Adsorption of methylene blue from aqueous solutions by synthetic montmorillonites of different compositions. *Glas. Phys. Chem.* **2016**, *42*, 207–213. [CrossRef]
39. Alikina, Y.A.; Kalashnikova, T.A.; Golubeva, O.Y. Sorption capacity of synthetic aluminosilicates of the kaolinite group of various morphology. *Glas. Phys. Chem.* **2021**, *47*, 42–48. [CrossRef]
40. Chaari, I.; Fakhfakh, E.; Medhioub, M.; Jamoussi, F. Comparative study on adsorption of cationic and anionic dyes by smectite rich natural clays. *J. Mol. Struct.* **2019**, *1179*, 672–677. [CrossRef]
41. Nogueira, F.G.; Lopes, J.H.; Silva, A.C.; Gonçalves, M.; Anastácio, A.S.; Sapag, K.; Oliveira, L.C. Reactive adsorption of methylene blue on montmorillonite via an ESI-MS study. *Appl. Clay Sci.* **2009**, *43*, 190–195. [CrossRef]
42. Chen, G.; Pan, J.; Han, B.; Yan, H. Adsorption of methylene blue on montmorillonite. *J. Dispers. Sci. Technol.* **1999**, *20*, 1179–1187. [CrossRef]
43. Krishna Kumar, A.S.; Warchol, J.; Matusik, J.; Tseng, W.L.; Rajesh, N.; Bajda, T. Heavy metal and organic dye removal via a hybrid porous hexagonal boron nitride-based magnetic aerogel. *NPJ Clean Water* **2022**, *5*, 24. [CrossRef]
44. Markelov, D.A.; Nitsak, O.V.; Gerashchenko, I.I. Comparative study of the adsorption activity of medicinal sorbents. *Pharm. Chem. J.* **2008**, *42*, 405–408. [CrossRef]
45. Rahimi, M.; Vadi, M.J. Langmuir, Freundlich and Temkin Adsorption Isotherms of Propranolol on Multi-Wall Carbon Nanotube. *Mod. Drug Discov. Drug Deliv. Res.* **2014**, *1*, 2348–3776.
46. Dada, A.O.; Olalekan, A.P.; Olatunya, A.M.; Dada, O.J.I.J.C. Langmuir, Freundlich, Temkin and Dubinin–Radushkevich isotherms studies of equilibrium sorption of Zn^{2+} unto phosphoric acid modified rice husk. *IOSR J. Appl. Chem.* **2012**, *3*, 38–45.
47. Ayawei, N.; Ebelegi, A.N.; Wankasi, D. Modelling and interpretation of adsorption isotherms. *J. Chem.* **2017**, *2017*, 3039817. [CrossRef]
48. Hu, Q.; Zhang, Z. Application of Dubinin–Radushkevich isotherm model at the solid/solution interface: A theoretical analysis. *J. Mol. Liq.* **2019**, *277*, 646–648. [CrossRef]
49. Revellame, E.D.; Fortela, D.L.; Sharp, W.; Hernandez, R.; Zappi, M.E. Adsorption kinetic modeling using pseudo-first order and pseudo-second order rate laws: A review. *Clean. Eng. Technol.* **2020**, *1*, 100032. [CrossRef]
50. Ho, Y.S.; McKay, G. Sorption of dye from aqueous solution by peat. *Chem. Eng. J.* **1998**, *70*, 115–124. [CrossRef]
51. Golubeva, O.Y.; Alikina, Y.A.; Brazovskaya, E.Y.; Vasilenko, N.M. Adsorption Properties and Hemolytic Activity of Porous Aluminosilicates in a Simulated Body Fluid. *ChemEngineering* **2022**, *6*, 78. [CrossRef]